CDA ACB
CANADIAN DAM ASSOCIATION
ASSOCIATION CANADIENNE DES BARRAGES

CDA 2012 Annual Conference
Congrès annuel 2012 de l'ACB
Saskatoon, SK Canada
September 22-27, 2012
du 22 au 27 Septembre 2012

DAM INFRASTRUCTURE FIRST INSPECTION SUPPORTED BY AN INTEGRATED MULTIBEAM ECHOSOUNDER (MBES) / LIDAR SYSTEM

Mathieu Rondeau, CIDCO, Rimouski (QC), Canada
Elisabeth Leblanc, CIDCO, Rimouski (QC), Canada
Luc Garant, AXSUB, Rimouski (QC), Canada

ABSTRACT

This paper's main purpose is the proposal of a new method to support the establishment of a first structural diagnosis that helps managers in their decision making process regarding maintenance on dam walls. Our approach bids on the quick and complete scan of the whole infrastructure through an integrated MBES / lidar system. The evaluation of the resulting dataset, according to the criteria of accuracy, uncertainty, resolution and density validates the performance of the proposed hybridized capture solution.
Armed with a series of value-added products such as deformation maps, acoustic backscatter maps or vertical and longitudinal profiles, managers can get an idea of the overall condition of the infrastructure they are responsible for. They can thus better plan maintenance work and focus divers' interventions and complementary technologies deployment only on problematic areas.

RÉSUMÉ

L'objet de cette communication tient dans la proposition d'une nouvelle méthode pour supporter l'établissement d'un premier diagnostic structural complet à l'intention des gestionnaires responsables de l'intégrité d'un mur de barrage. L'approche présentée mise sur le balayage rapide et complet de l'ensemble de l'infrastructure à l'étude par l'entremise d'un système intégré MBES / lidar. L'évaluation du jeu de donnée résultant, suivant les critères de précision, d'incertitude, de résolution et de densité valide la performance de la solution de captage hybridée proposée.
Avec en main une série de produits à valeur ajoutée qui prennent la forme de cartes de déformation, de cartes de réflectivité ou de profils longitudinaux et verticaux, le gestionnaire peut se faire une idée de l'état général de l'infrastructure dont il a la charge. Il peut mieux planifier les travaux d'entretien et concentrer les interventions de plongée et le déploiement de technologies complémentaires seulement sur les zones problématiques.

1 INTRODUCTION

Consider yourself for a moment as the manager in charge of the maintenance and the integrity of a dam, with all the responsibilities that come along with this role. What would you like to know? You would like to be aware of the general state of the infrastructure (above and below the waterline), to know where its possible weaknesses are, to assess the extent of potential damage, to monitor temporal structural deformations, all that in order to best organize the necessary work. In addition, you would like to be able to perform this analysis with minimal group closures or shutdowns of plants.

Traditionally, the inspection of underwater sections is visual and/or tactile and carried out by divers, but more often for security issues by Remotely Operated Vehicles (ROVs). Two major constraints, however, limit such interventions: low visibility and lack of precise positioning.
Poor visibility often requires the diver or ROV, equipped with optical camera, to carry out the examination by standing very close to the infrastructure, greatly increasing the time of inspection.

For its part, the lack of precise positioning prevents the mosaicking of all the images coming from the visual inspection and therefore the production of a global map of the infrastructure. Structural defects are then incorrectly set, global deformations are not detected and mostly, a recurring inspection, which finds its added value when always based on the same framework, is compromised. The georeferencing issue has recently being addressed by Ridao *et al.* (2010) with the deployment of a sophisticated ROV accurately positioned by using a USBL and a suite of onboard sensors (MRU + FOG, DVL) which allowed after a 30min mission the collection of a series of nearly 2000 images precisely georeferenced. These images were then stitched together into a high quality photo mosaic showing a 40m^2 section of the dam wall inspected.

In recent years, in response to the visibility difficulties encountered by divers and ROVs in the context surrounding infrastructures inspection, the use of acoustic technologies has emerged naturally. Several tests have been conducted with: mechanical scanning sonars (e.g. Clarke, 2006; Groupe Océan, 2007; Kongsberg, 2010; Abbott, 2011; Port de Montréal, 2011), side-scan sonars (e.g. Woo, 2007; Tritech, 2012), acoustic cameras (e.g. Brahim *et al.*, 2008) or even underwater laser scanners (e.g. Gillham, 2011).
All of these technologies remain limited by precise positioning achievement difficulties and, except for side-scan sonar, by short range constraint which results in time-consuming and laborious inspection. In quay wall inspections, the Port of Montreal and Groupe Océan have been successful in overcoming the georeferencing issue of a MS1000 mechanical scanning sonar by using complex deployment strategies (see Figure 1). However, such strategies seem difficult to transpose to the scale of a dam wall.

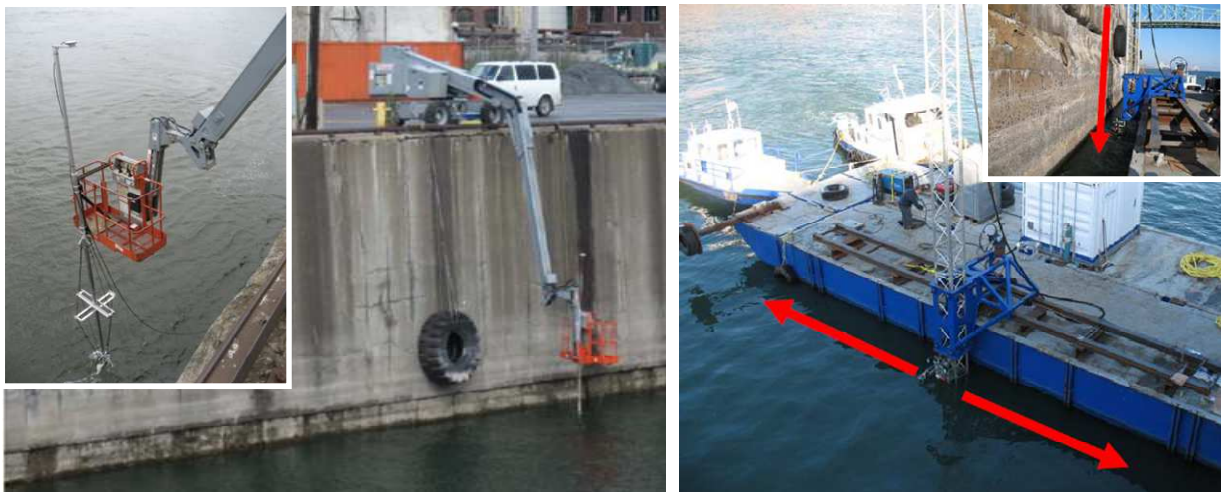

Figure 1: Deployment of a mechanical scanning sonar Kongsberg MS1000 at Port of Montreal. On the left side from a telescopic boom designed by the port authority and on the right side from a barge, with a rail system, designed by Groupe Océan.

Whether visual or acoustic, available technologies show a good inspection potential for the detection of rather thin structural defects. However, recognizing their respective limitations, these technologies would benefit from being deployed only sporadically in very specific places of the structure where a fine inspection seems necessary. This communication finds its main contribution in proposing and seriously evaluating a new survey method for accurately highlighting problematic areas of an infrastructure and thereby help managers to better plan divers' interventions and complementary technologies deployment.

Like the Port of London (Dillon-Leetch, 2008) and the Port of Marseille (Fraleu, 2006), we use a multibeam echo sounder (MBES) for the inspection of underwater sections. We improved the system by using a lidar for

the inspection of terrestrial (above water) sections. The two sensors mounted on a hydrographic survey vessel can get a full scan of the infrastructure. Beyond the classical 3D point cloud representation of the scanned infrastructure, we propose to provide managers with a range of 2D products suitable for informed decision making.

We will begin by presenting the technology mobilized, i.e. the instruments used and the deployment methodology. Different visualization products will then be presented. We will rely on the results of the ports of Montreal and Rimouski to discuss the performance of the technology in terms of accuracy, uncertainty, resolution and density. We will conclude by recalling the benefits of the proposed inspection method as well as with the short-term future developments to be carried out.

2 DEPLOYED SYSTEM

The system deployed for the dataset capture (Figure 2) is composed of: 1) a pole-mounted Reson Seabat 7125SV MBES tilted 30° on the starboard side, 2) an Applanix PosMV320 position and orientation unit, 3) a Terrapoint ALMIS-350 integrated system (Newby and Mrstik, 2005) composed of a Riegl Q-140 lidar, a NovAtel GPS antenna, and a Honeywell HG1700 inertial motion unit. The lever arms and the mounting angles between the different sensors have been accurately measured by a dimensional control survey of the vessel done with a total station.

Figure 2: Integrated MBES / lidar system mounted on the CIDCO's survey vessel.

The acquisition of bathymetric and topographic data is planned using a survey simulator that allows us, depending on customer expectations, to determine the number of passes required, the distance to the infrastructure, the survey speed and the optimal acquisition parameters.

3D centimetric positioning is ensured by RTK (Real Time Kinematic) differential correction from a GNSS receiver located close to the infrastructure. Raw GPS data are collected for possible post-processing with the Applanix Pospac MMS software which targets the generation of a PPK (Post Processing Kinematic) solution.

3 RESULTS AND PRODUCTS

3.1 3D models

Following the acquisition, the bathymetric and topographic datasets are individually processed. The two resulting 3D point clouds are then merged into a unified model. Figure 3 shows some examples of 3D models obtained on various structures.

The 3D model gives managers, for the first time, the ability to "see" in its entirety the infrastructure they are responsible for. However, the exploration of the 3D model does not yet fit in the habits of managers, even in those of engineers. Both are more comfortable with two dimensional datasets. That is why, beyond the production of a 3D model, derivative products have been imagined.

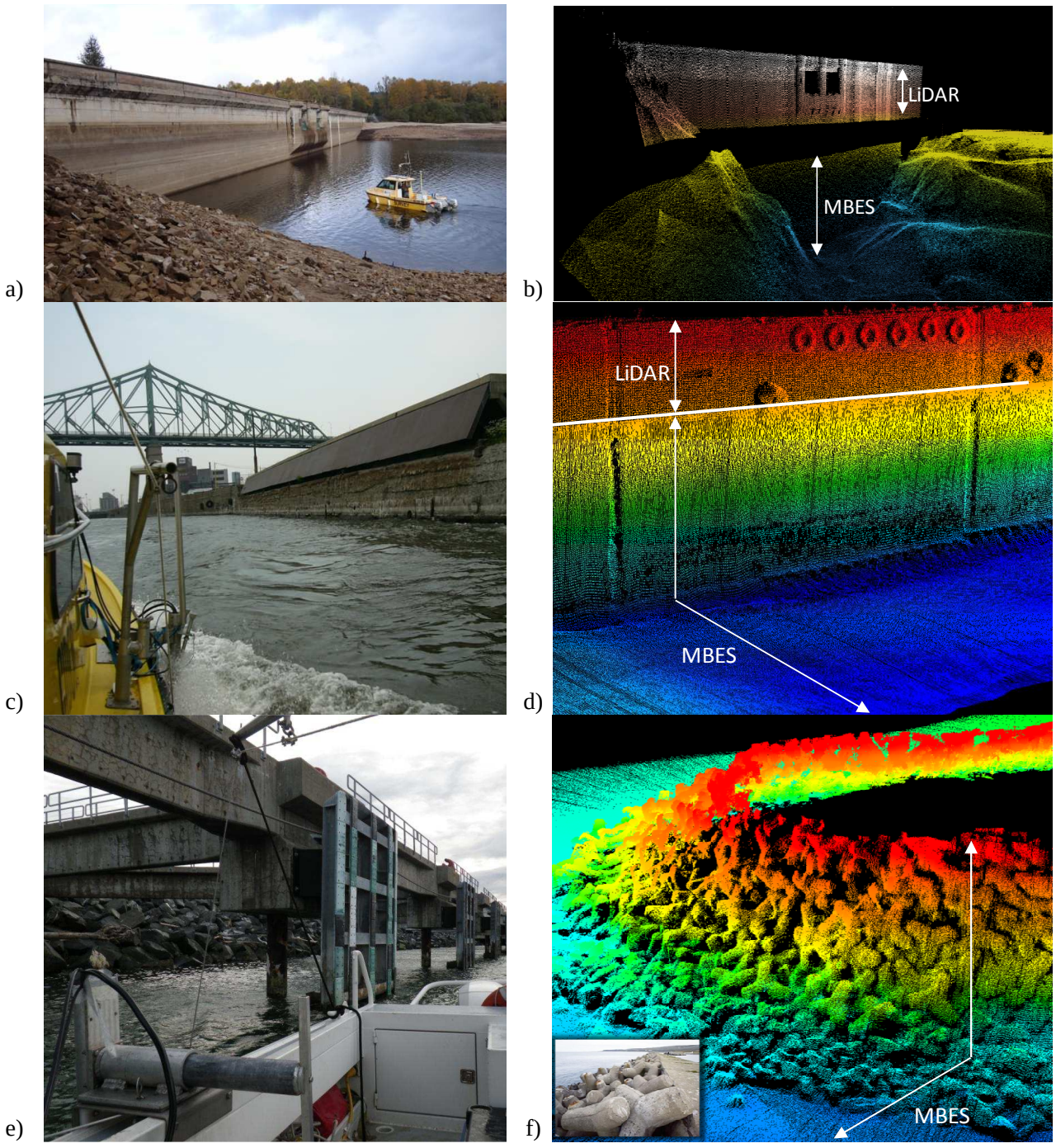

Figure 3: Example of 3D models from different structures. a) Survey of the Vassivière dam wall (France); b) unified 3D model; c) Survey of a quay wall section at the Port of Montreal; d) unified 3D model; e) Survey of a breakwater at the Port of Matane; f) 3D model (underwater section only).

The 3D model can so be declined, depending on the needs, in a vertical digital terrain model (VDTM) of the infrastructure, in a deformation map, in an acoustic backscatter map or in a series of longitudinal and transverse profiles.

3.2 Vertical digital terrain models and deformation maps

The VDTM (Figure 4 a)), but even more the five colors deformation map (Figure 4 b)), help managers to quickly give a first assessment of the infrastructure's general state. For example, the images below will help to monitor the concrete wall resurfacing degradation of a quay wall section at Port of Montreal. For managers who know the history of interventions already carried out, the analysis is even more evident.

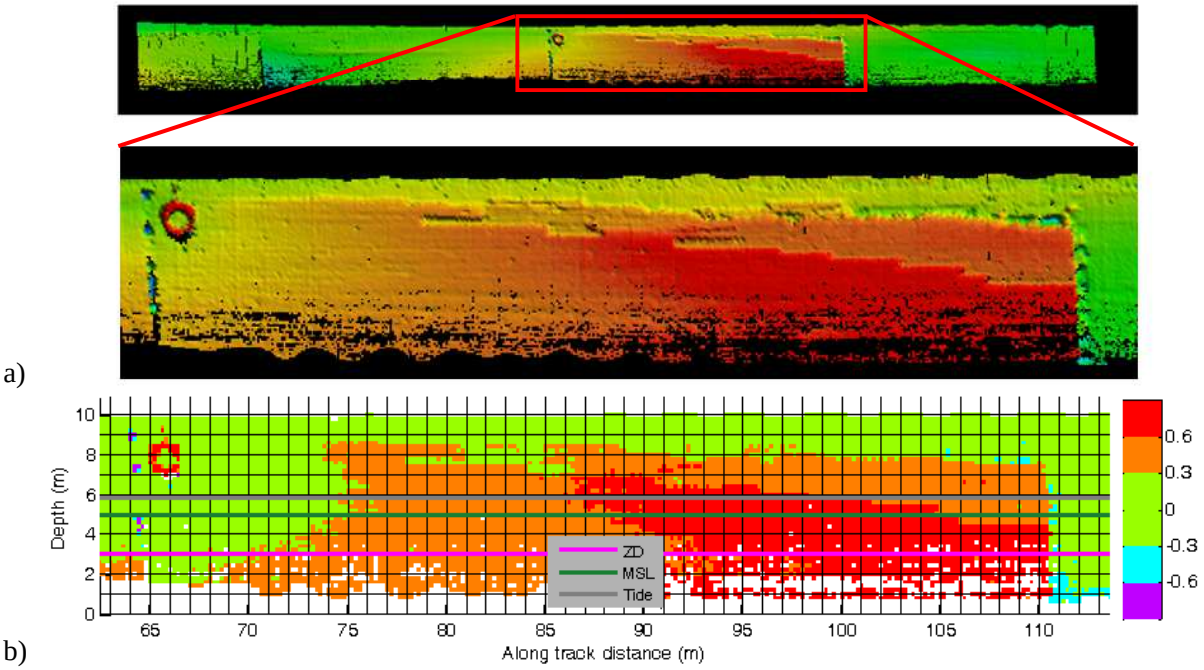

Figure 4: a) Vertical digital elevation model of a quay wall section at the Port of Montreal; b) Five colour deformation map. The colour scale goes from green (no deformation compared to the theoretical structure's position) to purple (more than 60 cm of gouging) and to red (more than 60 cm of protruding).

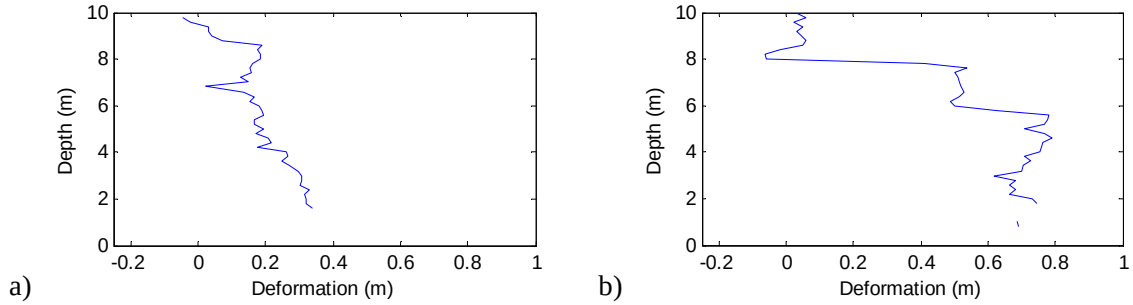

Figure 5: Vertical profiles from a quay wall section at the Port of Montreal. a) 70 m along track; b) 100 m along track.

The deformation map is produced with respect to a theoretical vertical plane. Year after year, because the georeferencing is accurately managed, it is possible, by referring always to the same plan, to monitor temporal structural deformations of the infrastructure, such as undermining, gouging or protruding effects.

3.3 Acoustic backscatter maps

The acoustic backscatter map represents the intensity of the acoustic return measured on the infrastructure. Such an image should, in theory, highlight changes in textures of materials (wood, concrete, steel) making up the infrastructure, each responding differently to acoustic excitation. Work on the subject is in progress.

3.4 Profiles

Profiles (longitudinal and transverse) are currently the product structural engineers are more used to working with. It mainly allows the detection of a loss of verticality of the structure. Figure 5 shows 2 examples of such vertical profiles at the Port of Montreal. We can see in a) that the structure at 70 m along track is in much better conditions than at 100 m along track in b).

4 PERFORMANCE AND LIMITS

We have seen in the previous section that it is possible to create products that are visually evocative and easy to use from the combined MBES / lidar datasets. It is however important to assess the quality of the data that was used to derive those products. The main questions we want to answer about the original 3D points cloud are:

- What is the accuracy, or how far off is the measurement from reality?
- What is the uncertainty, or the maximum range of values that would outcome after scanning the same point repeatedly?
- What is the resolution, or the smallest difference in morphology, that can be detected?
- What is the density, or how many points do we get per square meter?

4.1 Accuracy

Assessing the accuracy of a system comes down to determining if there is a constant offset between the measurements and reality. To test the accuracy of our system, we surveyed a quay wall section at the Port of Montreal using both a robotic total station (known to have a very high accuracy) and our integrated MBES / lidar system. The survey area was located in the tide zone providing a 1m overlap between the sonar and the total station and a 2.5m overlap between the lidar and the total station, as shown in Figure 6.

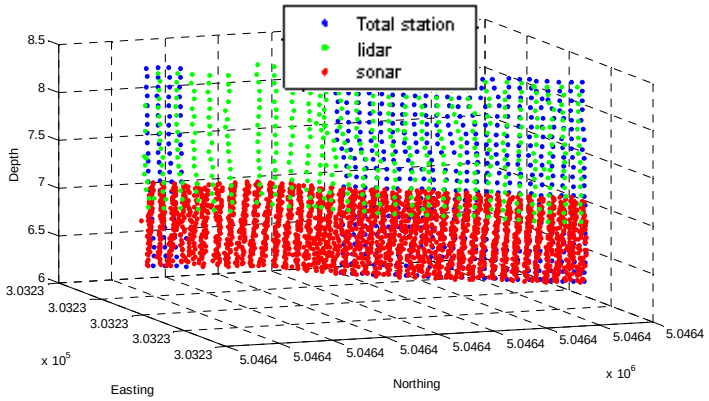

Figure 6: Quay wall section studied at the Port of Montreal for accuracy assessment.

First, the sonar and lidar datasets were manually edited to remove any gross errors that would also be deleted to create one of the derived products shown earlier. Then, for each sonar and lidar point, the 3 closest points from the total station were located and a plane fitting was performed. The orthogonal distance was then calculated between the sonar or lidar point and the plane. The mean orthogonal distance is used to measure accuracy. Values of -4.52 and 2.23 cm were found for the sonar and the lidar respectively. This implies that the sonar tends to underestimate the distance to the surface and the lidar, to overestimate it. More tests will have be done to see if those offsets are consistent over different surveys and intrinsic to the systems, in which case, they could simply be removed. If it is not the case, better calibration methods will be investigated.

4.2 Uncertainty

Although some models do exist to predict the uncertainty of our datasets, it is a criterion that is highly environmentally dependent as it increases with background noise. The mathematical definition of uncertainty can vary from one source to the other. Here we are taking a 95% confidence interval. In other words, an uncertainty of u cm would mean that 95% of the measures of x would fall between $x_{ref} - u$ and $x_{ref} + u$, where x_{ref} is a reference value:

$$u = 1.96\sqrt{\frac{\sum\left(x - x_{ref}\right)^2}{N-1}} \qquad (1)$$

The datasets from the Port of Montreal corrected for gross errors were also used to get an estimate of uncertainty for the sonar and lidar using the total station as reference (x_{ref}). The results were 6.76 and 5.47 cm for the sonar and the lidar respectively.

However, it should be noted that uncertainty should be estimated on a flat surface, otherwise edge effects can bias the results. The surface used from the Port of Montreal had a deformation range of about 25 cm (see Figure 7 a).

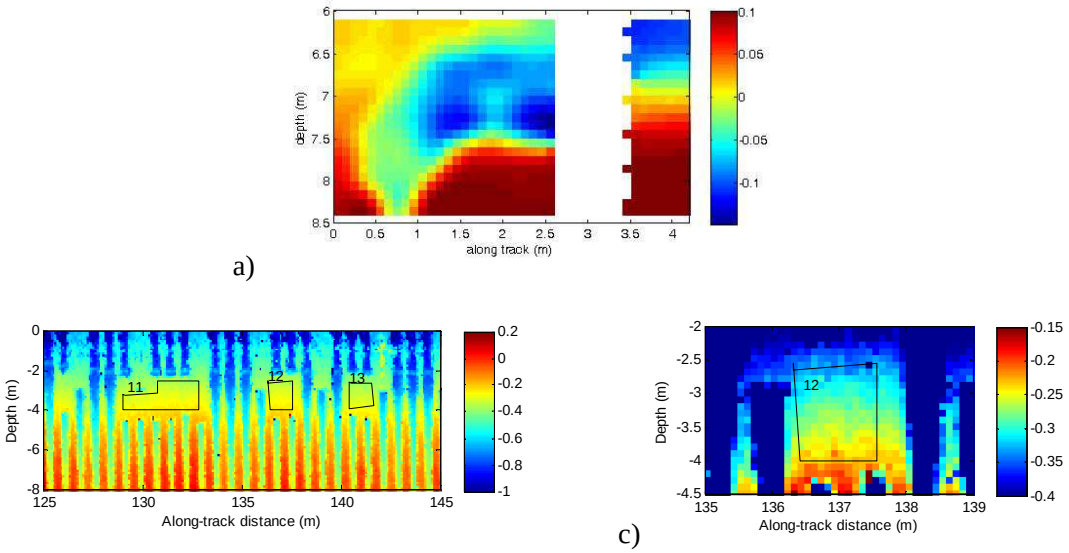

a)

b)

c)

Figure 7: Surfaces studied for uncertainty assessment. a) Total station in Port of Montreal; b) high density flat sonar surfaces in Port of Rimouski; c) zoom of b). The colour range is different for each image to highlight the relevant information.

These drastic changes can result in overestimating the uncertainty. To validate this hypothesis, we isolated 22 flat areas from a sonar dataset acquired in Port of Rimouski such as those shown in Figure 7 b). We can see on the zoomed area in Figure 7 c) that the deformation range is much lower, around 10 cm. Since no total station datasets were available for this structure, we took advantage of the fact that the surface was surveyed with high redundancy (4 passes) to create smoothed reference surface using the software CARIS HIPS & SIPS 7.1.1. Each sonar point was then compared to the value of the closest node in the reference surface and the uncertainty was computed using (1). The results show an overall uncertainty of 3.93 cm, almost half of the one estimated in Port of Montreal. This improvement is due in part to the surfaces being more flat, but also possibly to the fact that better settings were used on the sonar and the survey distance to the surface was about 10 m in Rimouski compared to about 15 m in Montreal. The 3.93 cm uncertainty is therefore more realistic for future work since a closer distance and the new settings will be used. A similar approach will have to be tested with the lidar to see if the uncertainty decreases in the same way.

4.3 Resolution

It is not an easy task to measure the resolution of a sonar system experimentally because it implies mooring controlled targets of different sizes. This issue will be addressed in the next phase of the project, but in the meantime, we can still look at the theoretical resolution calculated by the survey simulator mentioned earlier. The work of Lurton (2002) served as a basis to derive the equations used in this section. The resolution of the sonar is given by 3 different values corresponding to the x (along-track), y (across-track) and z (vertical) axis (see Figure 10). For each axis, up to 3 components must be taken into account: the resolution due to the pulse length, to the sampling rate and to the beam footprint. The effective resolution is the most penalizing of the 3 components. The values given in the present section will assume a flat surface, a depth D of 8 m, a distance d between the vessel and the structure of 10 m, a sound velocity c of 1500 m/s and a pulse length T of 33µs.

The along-track resolution, dx, is only determined by the size of the beam footprint along the x axis (see Figure 8 a) and b)). The size of the footprint varies in function of the along track beamwidth angle θ_x and the beam angle θ, which is a function of depth D and distance d from the vessel to the structure:

$$dx_{foot} = 2Rtan\left(\frac{\theta_x}{2}\right) \quad (2)$$

$$R = \sqrt{D^2 + d^2} \quad (3)$$

When using 512 beams, the Reson Seabat 7125 has an along-track beamwidth of 1°. We can see in Figure 9a) that the along-track resolution worsens with depth.

The across-track resolution, dy, has a time sampling component and a pulse length component. The time sampling component is at best (if no averaging is performed in the bottom detection algorithm) given by the horizontal projection of the slant resolution dr due to time sampling (see Figure 10). It varies as a function of the beam angle θ:

$$dy_{Fs} = \frac{c}{2Fs} sin\theta \quad (4)$$

$$\theta = \text{atan}\left(\frac{D}{d}\right) \quad (5)$$

where *Fs* is the sampling rate. The sampling rate of the Reson Seabat 7125 is 34 kHz. The across-track resolution due to time sampling as function of depth is shown in red on Figure 9 b). We can see that this component improves with depth.

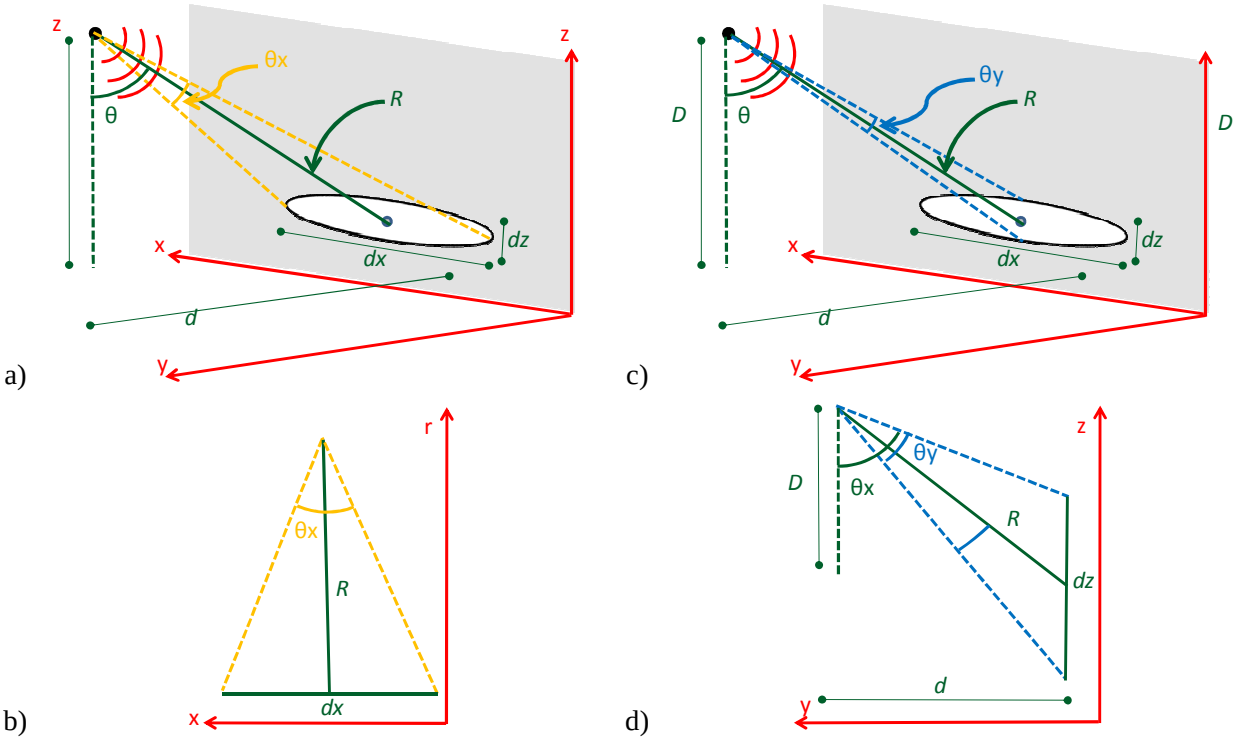

Figure 8: Resolution due to beam footprint. a)3D view of the along-track footprint; b)2D view of the along-track footprint. For better visualization, the *z* axis has been replaced by *r*, an axis parallel to the range *R*; c)3D view of the across-track footprint; d)2D view of the across-track footprint.

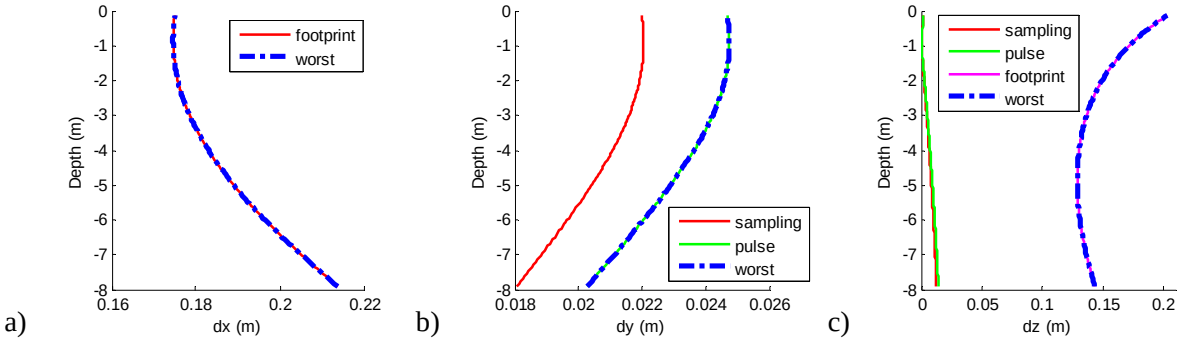

Figure 9: Sonar resolution as function of depth. a)Along-track resolution; b)Across-track resolution; c)Vertical resolution.

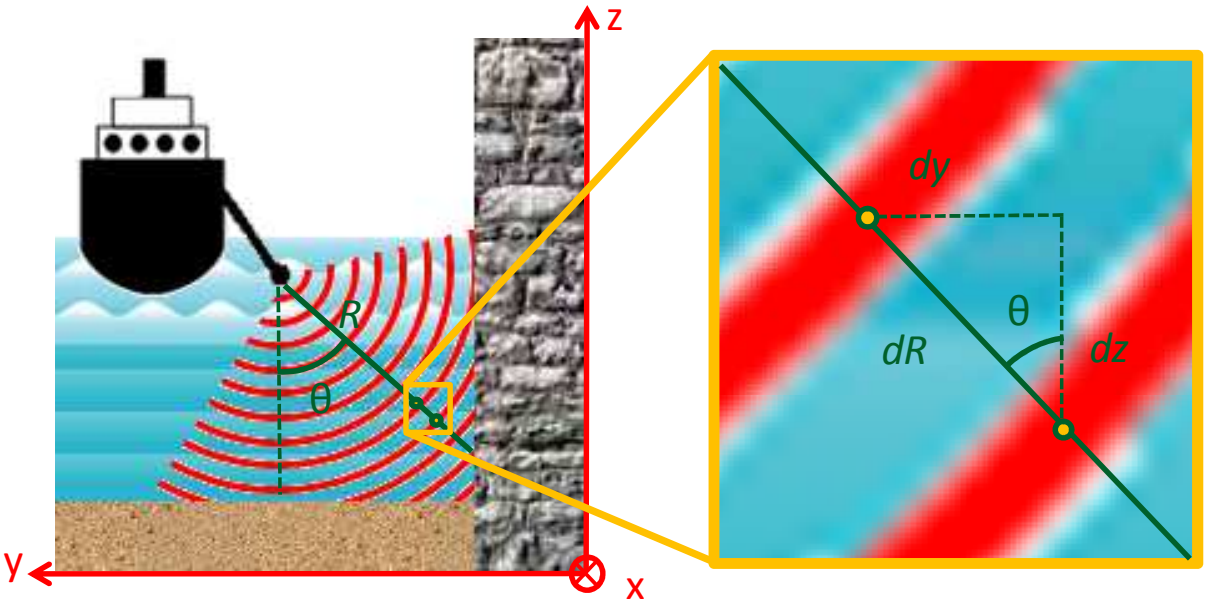

Figure 10: Resolution due to time sampling

The pulse length component is due to the fact that two echoes can only be distinguished if they are at least half a pulse length apart. This lead to a time resolution that can be transposed in range and projected along the *y* axis:

$$dy_T = \frac{c}{2T} sin\theta \quad (6)$$

We can see on Figure 9 b) that this component follows the same tendency as the time sampling, but is more limiting.

Finally, the vertical resolution is limited by the footprint, the time sampling and the pulse length. The footprint geometry is shown on Figure 8 c) and d). The footprint resolution can be computed using:

$$dz_{foot} = \frac{d}{cos\left(\theta + \left(\frac{\theta_z}{2}\right)\right)} + \frac{d}{cos\left(\theta - \left(\frac{\theta_z}{2}\right)\right)} \quad (7)$$

The time sampling and pulse length component are similar to those computed along across-track, but are projected vertically:

$$dz_{Fs} = \frac{c}{2Fs} cos\theta \quad (8)$$

$$dz_T = \frac{c}{2T} cos\theta \quad (9)$$

We can see on Figure 9c) that the footprint component is definitely dominant along *z*.

Overall, we can say that under the conditions described at the beginning of the section, the sonar would be able to represent defects that are of the order of 19x2x15 cm.

4.4 Density

The last quality criterion is the density. It is important because even with an excellent resolution, one would not be able to distinguish defects in the structures if not enough points are collected per area. Density was analyzed both theoretically using the simulator and experimentally at Port of Rimouski.

The density of points depends on the number of passes *n*, the average distance between two soundings along-track (Δx) and vertically (Δz).

$$\rho = \frac{n}{\Delta x \Delta z} \quad (10)$$

Along-track, this distance decreases with the ping rate and decreases with the vessel speed, but is not influenced by depth:

$$\Delta x = \frac{v}{PR} \quad (11)$$

The vertical distance between the beams depends on the configuration of the sonar during acquisition. Using the equi-angular mode that spreads the beams with a constant angular opening, and realistic survey parameters (vessel speed of 3.86 knots, ping rate of 21.1, 4 passes) we can see that the distance between the beams increases with depth (see Figure 11 a)) and the density decreases accordingly (see Figure 11 b)).

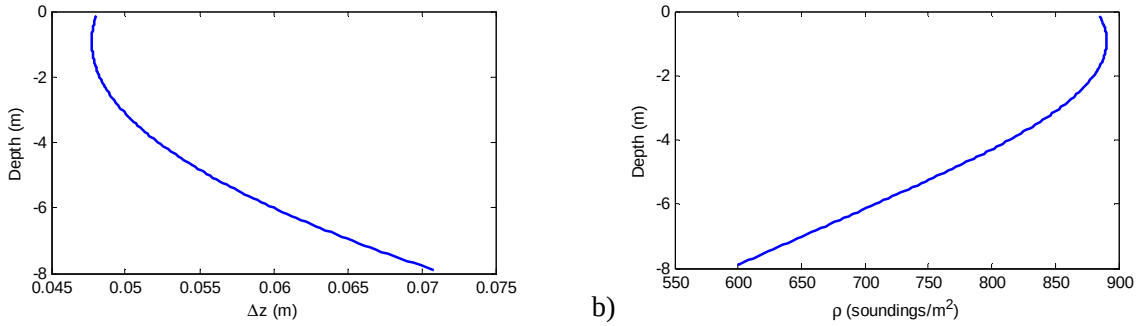

Figure 11: Theoretical density as function of depth. a)Vertical distance between the beams; b)Density.

To validate the density calculated by the simulator, we analyzed the dataset from Port of Rimouski. The structure was divided into depth layer of 20 cm and the number of soundings for each layer was divided into the corresponding area in square meters. The results appear in blue on Figure 12 a) along with the theoretical curve in red. The difference between both curves is shown on Figure 12 b). We can see that the general tendency is respected, except at the bottom where soundings from the seafloor contributed to increase the density. However, we recorded in practice around 200 soundings (or one quarter) less then what was predicted. Manual editing contributed to decrease the number of soundings, but not enough to explain the difference observed. A better explanation is the morphology of the surface. The wharf studied is made out of sheet piling as shown on the left of Figure 13 a). This type of structure produces an acoustic shadow effect: the bulges are hiding the cavities next to them and the sonar cannot insonify these areas. This effect is illustrated on Figure 13. We can see on the density map in b) some vertical stripes of lower density. They are located precisely on the left of the bulges shown on the deformation map in c).

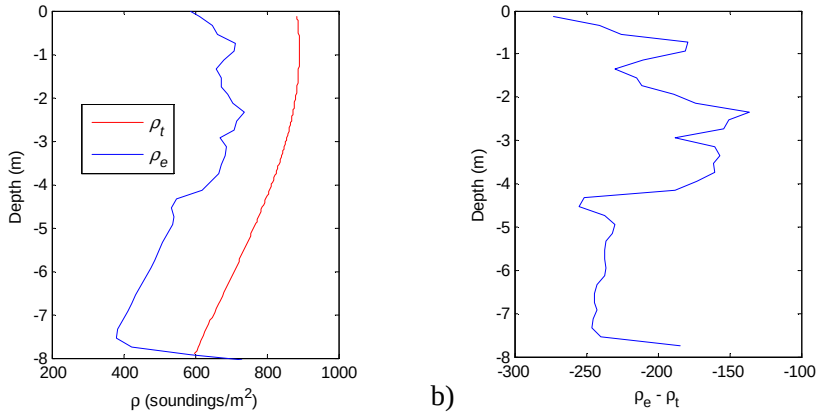

a) b)

Figure 12: Theoretical vs. experimental density as function of depth. a) Comparison between theoretical (ρ_t) and experimental (ρ_e) density. b) Difference between ρ_t and ρ_e.

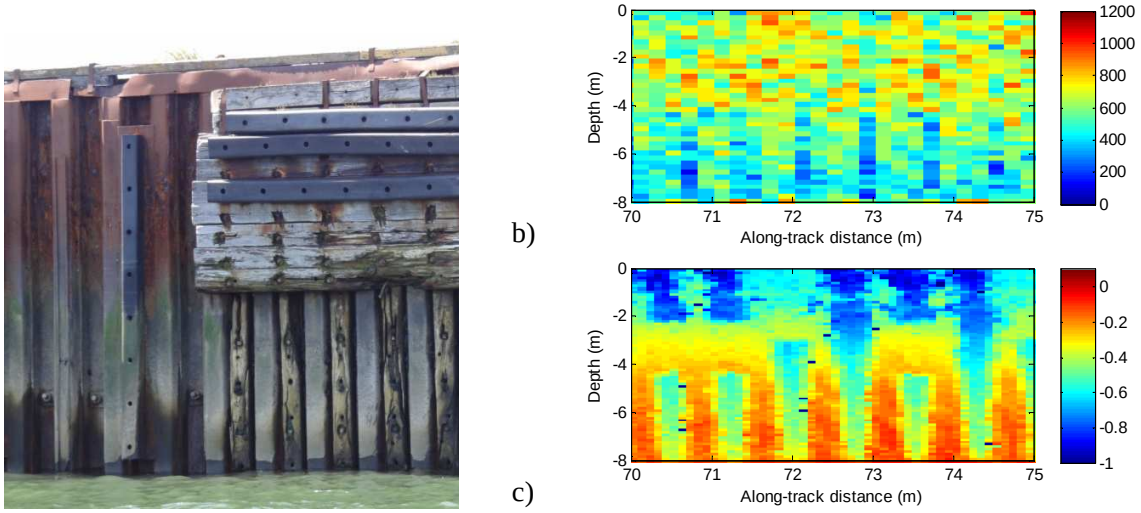

a) b) c)

Figure 13: Density and deformation. a) Wharf made out of sheet piling; b) Density (soundings/m^2) map; c) Deformation map for the same area (m).

5 CONCLUSION

The proposed approach suggests that prior to any intervention on a partially wet infrastructure (dam wall, quay wall, bridge pier), a first overall structural picture should be taken at a point in time in order to help managers to better plan maintenance programs and in-situ interventions (like divers or complementary technologies deployment). To achieve such a first diagnostic, CIDCO has proposed and seriously evaluated a new survey method based on a hybridized MBES / lidar capture solution to quickly obtain a complete (underwater and terrestrial sections) and accurate (<5cm uncertainty) 3D model of an infrastructure at a decimetre resolution.
In light of the results obtained on several survey sites in the province of Quebec, infrastructure inspection companies (mainly diving companies) agreed that a paradigm shift is taking place and began to express their interest in the use of hybridized MBES / lidar capture solutions. Together with its partners, CIDCO is thus seeking an effective transfer mechanism to bring new technological solutions and methods to the infrastructure inspection market. A first initiative is the creation of an infrastructure inspection expertise centre in Rimouski

(Quebec). The expertise centre's objectives would be to: 1) intensify R & D efforts already undertaken and allow Canadian companies to remain well positioned on the international market; 2) establish a training centre to assist companies interested in taking control of new available inspection equipment; 3) develop a certification centre to assess the performance of new equipment and support the legitimacy of their use with clients.

6 REFERENCES

Abbott, B. (2011). "Visualization of underwater structures: Improving the safey of infrastructure." Journal of Ocean Technology 6(2): 1-8.

Brahim, N., S. Daniel and D. Guériot (2008). Potential of underwater sonar systems for port infrastructure inspection.

Clarke, R. (2006). Condition surveys of underwater infrastructure during full plant operations providing 2-D and 3-D representation. CDA 2006 Annual Conference, Québec city (QC).

Dillon-Leetch, J. (2008). High Resolution Hydrographic Surveying at The Port of London. Port&Terminal Technology Conference.

Fraleu, B. (2006). "Modélisation 3D au service de l'inspection d'ouvrages portuaires immergés." XYZ 109: 45-48.

Gillham, J., http://www.2grobotics.com/SonarAndLaserMeasuringComparison.pdf (10 Jan. 2012). (2011). "Underwater Sonar and Laser Measuring. An Experimental Comparison." Retrieved 10 Jan. 2012, from http://www.2grobotics.com/SonarAndLaserMeasuringComparison.pdf

Groupe Océan. (2007). from.http://www.groupocean.com/upload/services/presentation_generale_imagerie_port_de_montreal_1.pdf.

Kongsberg (2010). "MS1000 system successfully trialed at hydroelectric dam in Laos." The Subsea Newsletter 03/10: 4.

Lurton, X. (2002). An Introduction to Underwater Acoustics.

Newby, S. and P. Mrstik (2005). "LiDAR on the level in Afghanistan: GPS, Inertial map the Kabul Road." GPS World 16(7): 16-22.

Port de Montréal (2011). Intégration des données SONAR+LIDAR au système de gestion et inspection des quais du Port de Montréal (SGIQ), internal presentation.

Ridao, P., M. Carreras, D. Ribas and R. Garcia (2010). "Visual inspection of hydroelectric dams using an autonomous underwater vehicle." Journal of Field Robotics 27(6): 759-778.

Tritech. (2012). from http://www.tritech.co.uk/news-article/starfish-990f-side-scan-sonar-enhances-port-survey-operations

Woo, J. (2007). "Are the Bridge Piers Safe ? Submerged Pier Survey by Side-scan Sonar." Hydro International 11(11): 32-35.